Variable operation of a renewable energy-driven reverse osmosis system using model predictive control and variable recovery

Mito, Mohamed T.; Ma, Xianghong; Albuflasa, Hanan; Davies, Philip

DOI:
10.1016/j.desal.2022.115715

Document Version
Peer reviewed version

Citation for published version (Harvard):
Mito, MT, Ma, X, Albuflasa, H & Davies, P 2022, 'Variable operation of a renewable energy-driven reverse osmosis system using model predictive control and variable recovery: towards large-scale implementation', *Desalination*, vol. 532, 115715. https://doi.org/10.1016/j.desal.2022.115715

Supplementary material

Variable Operation of a Renewable Energy-Driven Reverse Osmosis System Using Model Predictive Control and Variable Recovery: Towards Large-Scale Implementation

Desalination

Mohamed T. Mito [a, d], Xianghong Ma [a], Hanan Albuflasa [b], Philip A. Davies *[c]

[a] Sustainable Environment Research Group, School of Engineering and Technology, Aston University, Birmingham B4 7ET, UK.

[b] Department of Physics, College of Science, University of Bahrain, P O Box 32038, Kingdom of Bahrain.

[c] School of Engineering, University of Birmingham, Edgbaston, Birmingham B15 2TT, UK.

[d] Mechanical Engineering Department, College of Engineering and Technology, Arab Academy for Science, Technology and Maritime Transport, Abu-Qir, Alexandria, Egypt.

*corresponding author: P.A.Davies@bham.ac.uk

S.1 Model validation

This section describes the model validation using measured data collected from the lab RO system. The model accuracy was assessed for predicting the permeate flowrate, brine flowrate, feed pressure, permeate concentration, and power consumption, for defined inputs, i.e., the HPP and iSave speeds, and input disturbances. The model steady-state output and dynamic response prediction accuracy are presented as follows:

S.1.1 Steady-state model validation

The steady-state model outputs were compared to measured data obtained with varying feed concentration (25,000 to 40,000 mg/l) and feed temperature (20 to 30ºC). The data were recorded and averaged for one minute after the permeate concentration stabilised, thus indicating that the system reached steady state. Details of the measuring instruments and experimental errors are described in Section S.2. The dataset, included in supplementary material 1 - Appendix C, was simulated using the RO model at the same inputs and disturbances and compared to the experimental data. A regression analysis showing the correlation between the experimental and simulated data is shown in Fig. S.1. The prediction accuracy was assessed using R^2 and RMSE, as summarised in Table S.1. The model showed high accuracy for predicting the permeate flowrate, brine flowrate, feed pressure and power presented by an R^2 of 0.93, 0.97, 0.98 and 0.99 and a RMSE of 0.253 m^3/h, 0.14 m^3/h, 1.124 bar and 0.303 kW, respectively. The prediction accuracy for the permeate concentration was more modest compared to other parameters, at an R^2 of 0.77 and RMSE of 70.145 mg/l, caused by an overestimation of the permeate concentration at low flowrates, as highlighted in Fig. S.1 (e). The model accuracy was also checked with ROSA to ensure the model validity for predicting the permeate concentration, in which a correlation of (R^2 = 0.97) between the model outputs and ROSA was achieved for the same inputs and disturbances.

Fig. S.2 compares the measured and simulated data of the feed pressure and power consumption for a specific permeate flowrate. The error between the measured and simulated feed pressure and power consumption remained below ±2.5% and ±4.7%, respectively. The estimated experimental error for the feed pressure and power consumption based on the accuracy of measuring instruments were 0.25% and 0.5%, respectively.

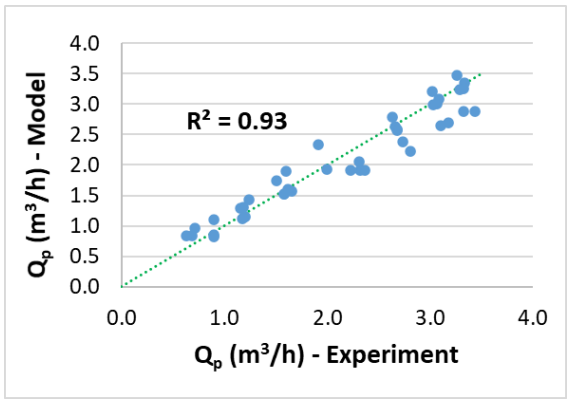

(a)

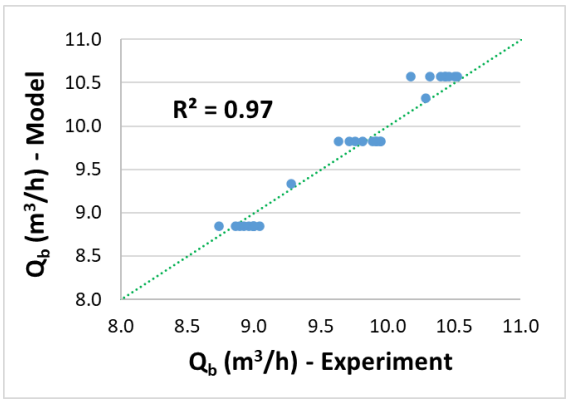

(b)

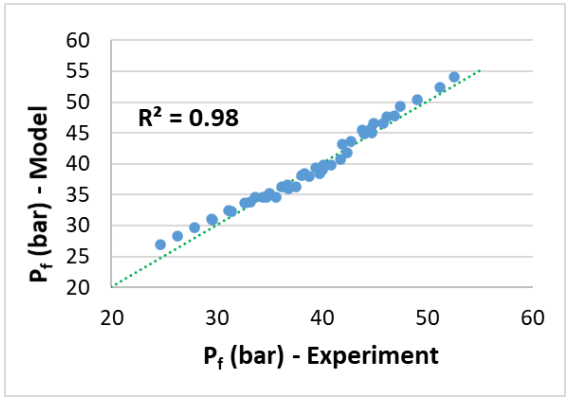

(c)

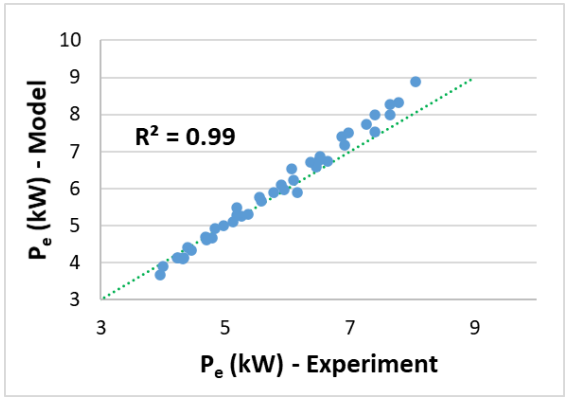

(d)

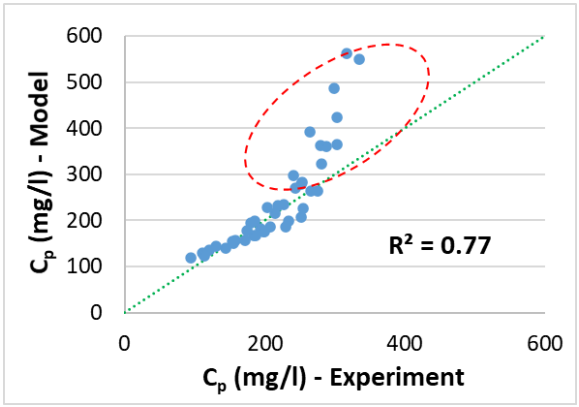

(e)

Fig. S.1. Regression analysis showing the correlation between the experimental and simulated data for the a) permeate flowrate, b) brine flowrate, c) feed pressure, d) power consumption and e) permeate concentration.

Table S.1.

Validation of the Steady-state model output represented by the coefficient of determination (R^2) and Root Mean Square Error (RMSE).

	Permeate flowrate (Q_p)	**Brine flowrate (Q_b)**	**Feed pressure (P_f)**	**Power ($P_{e,total}$)**	**Permeate concentration (C_p)**
Regression analysis	$R^2 = 0.93$	$R^2 = 0.97$	$R^2 = 0.98$	$R^2 = 0.99$	$R^2 = 0.77$
RMSE	0.253 m^3/h	0.14 m^3/h	1.124 bar	0.303 kW	70.145 mg/l

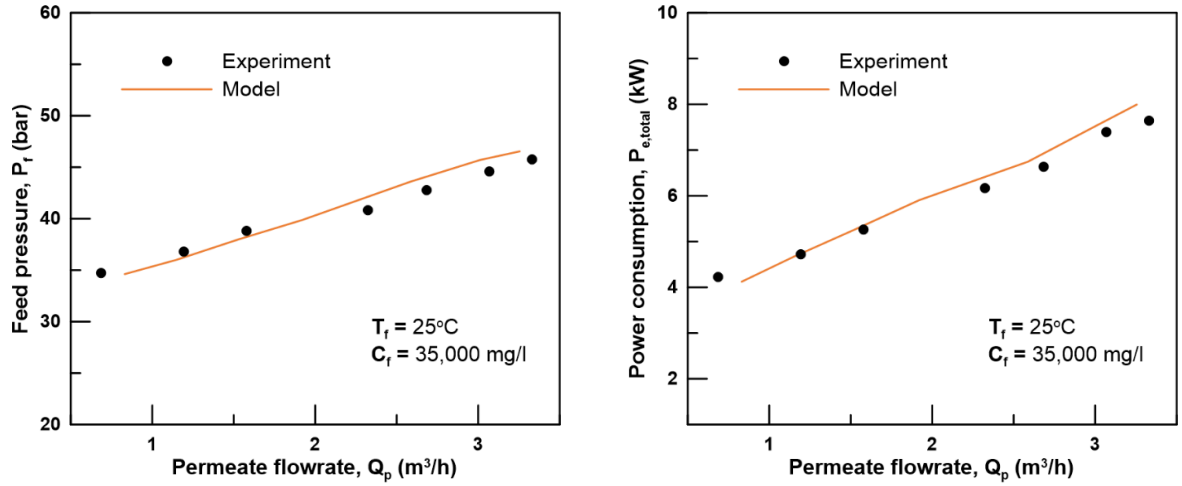

(a) (b)

Fig. S.2. A comparison between the measured and simulated a) feed pressure and b) power consumption for the same permeate flowrate. The data is collected at a feed concentration of 35,000 mg/l and a feed temperature of 25°C.

S.1.2 Dynamic model validation

The model prediction accuracy for the plant dynamic response was assessed by its ability to predict a transient change in permeate flowrate, feed pressure, and permeate concentration for a 10% step-change in the HPP rotational speed, N_{HPP}. Fig. S.3 presents the measured and simulated system response for a step-change in permeate flowrate. The model provided high accuracy in predicting the measured data, as the error remained within a ±5% margin along the step-test. The change in permeate production reached steady state almost instantly for the change in HPP speed. This was due to using a positive displacement HPP, where the pump discharge flow is directly proportional to the pump speed. The fluctuations in the measured

flow data were due to the sensitivity of the paddle-wheel flow sensor to any turbulence or pulsation in the flow stream.

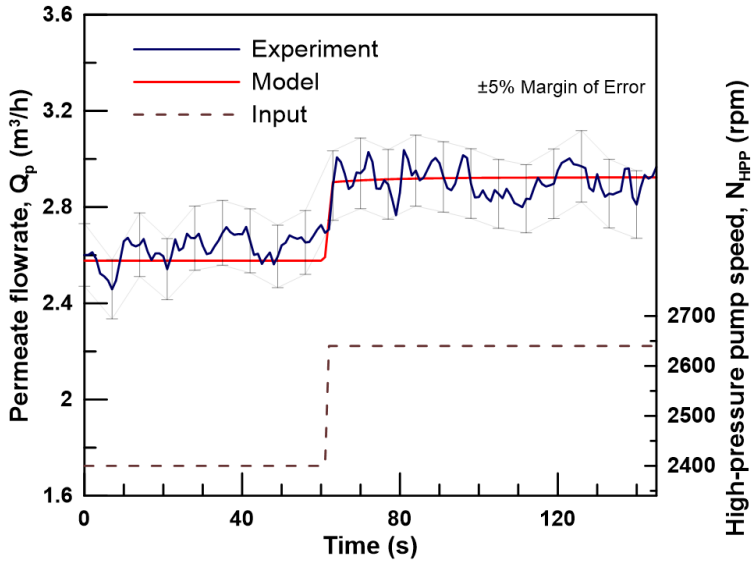

Fig. S.3. Validation of model accuracy for predicting the permeate flowrate dynamic response. The step-response test was performed at 28°C feed temperature and 35,195 mg/l feed concentration. The permeate recovery varied from 20.7% to 22.9%.

The model also delivered high accuracy when simulating the feed pressure. As shown in Fig. S.4, the measured and predicted data remained within a 3% error margin. The change in feed pressure due to a step-change in HPP speed exhibited two characteristic behaviours. Initially, the change in pressure was instantaneous in alignment with the change in HPP discharge flow and increased flow volume in the brine channel. The second part of the response, exhibiting the characteristics of a first-order system, was an osmotic pressure increase due to increased concentration and salt accumulation accompanying the increase in permeate flowrate.

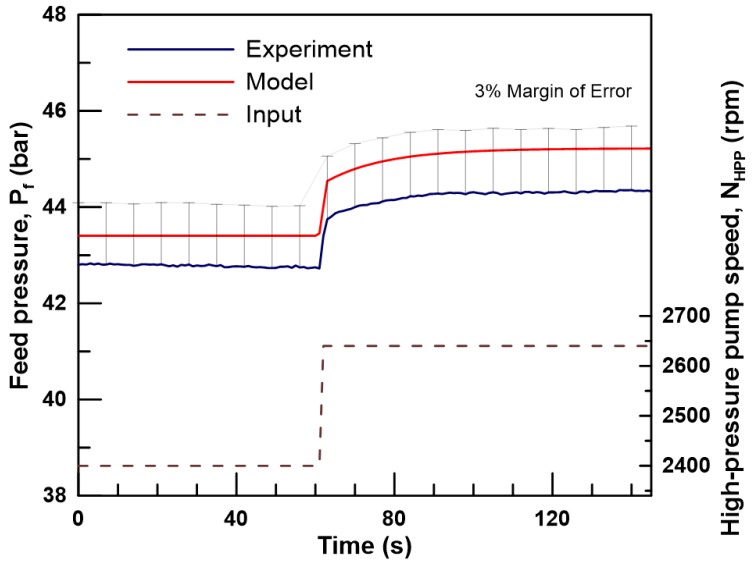

Fig. S.4. Validation of model accuracy for predicting the feed pressure dynamic response. The step-response test was performed at 28°C feed temperature and 35,195 mg/l feed concentration. The permeate recovery varied from 20.7% to 22.9%.

The comparison between the predicted and measured permeate concentration due to a step increase in HPP speed is presented in Fig. S.5. The model accurately predicted the decline in permeate concentration by approximating its response to a first-order system. The model showed high accuracy, such that the predicted and measured data remained within a 5% error margin. This confirmed the validity of the concentration conservation equations used in this study.

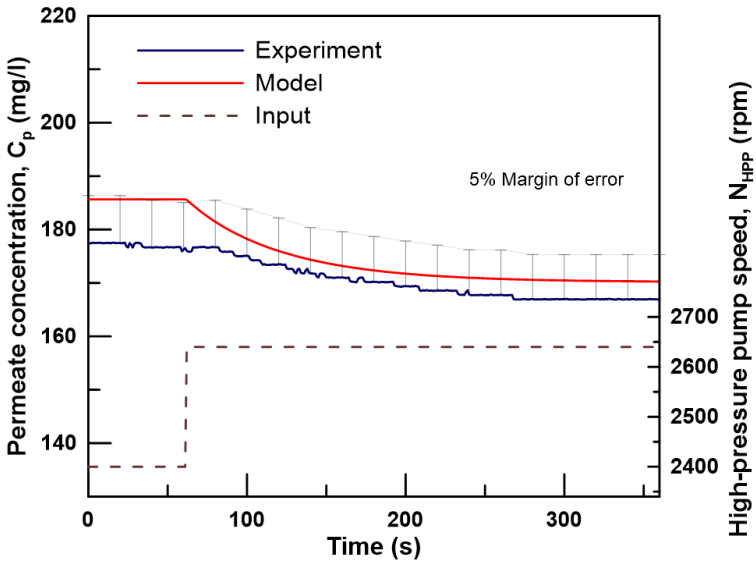

Fig. S.5. Validation of model accuracy for predicting the permeate concentration dynamic response. The step-response test was performed at 27°C feed temperature and 35,429 mg/l feed concentration. The permeate recovery varied from 20.7% to 22.9%.

S.2 Instrumentations and measurements

This section describes the instrumentations used for data collection. The RO system included 16 sensors distributed across the RO test-rig to collect data for flowrate, pressure, concentration, temperature, and power consumption. The sensors were compatible for use with seawater and were selected to meet the operating range of the physical variable to be measured. The voltage required to power the sensors was provided by an external 24V DC power supply. The sensors were connected in series with the power supply forming a loop, by which, the current signal within the loop ranges from 4 – 20 mA and represents the physical reading of the sensor. This configuration is referred to as a "Loop-powered" circuit. All the sensors, except the conductivity sensors, were factory calibrated.

S.2.1 Flow measurement

The flowrate for the feed, brine and permeate streams were measured using the FPB151 flowmeter manufactured by OMEGA (Manchester, United Kingdom), shown in Fig. S.6. It consists of a paddlewheel flowmeter mounted on a Tee and connected to a transmitter that converts the paddlewheel speed to a current signal representing the flow. The transmitter generated a 4 – 20 mA signal for a 0 - 30 m^3/h flow range with an accuracy of ± 1% of the max flowrate reading [1].

Fig. S.6. Paddlewheel flowmeter.

S.2.2 Pressure measurement

The pressure across the RO system was measured using the RS PRO IPS Series pressure sensors, shown in Fig. S.7, manufactured by RS components (Northants, United Kingdom). They are piezo-resistive ceramic sensors with a stainless-steel housing that generated a 4 - 20 mA signal with respect to their pressure range with an accuracy of ±0.25% of max value [2]. The sensors fitted on the LP piping were rated from 0 to 16 bar, while the sensors on the HP side were rated from 0 to 100 bar.

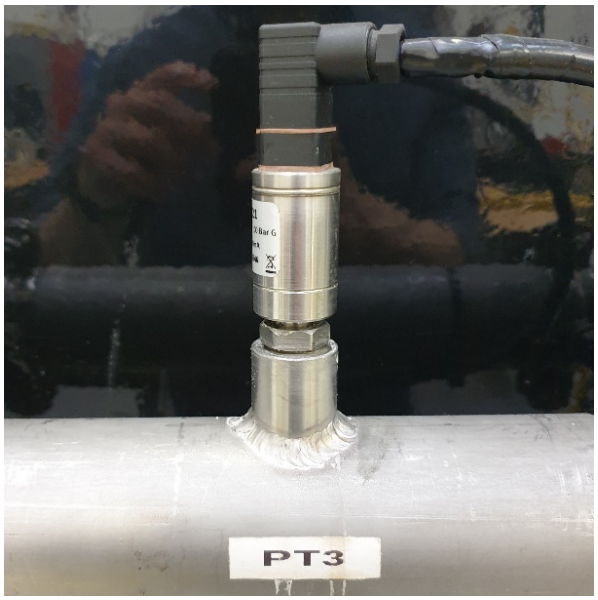

Fig. S.7. Pressure transmitter.

S.2.3 Concentration measurement

The feed and permeate concentration were measured using the OMEGA CDTX-2854 conductivity transmitter, shown in Fig. S.8. It is an integrally mounted conductivity sensor and transmitter that delivers an accuracy of ±2% of reading [3]. The sensors provided a conductivity reading of 0 to 5000 µS/cm and 0 to 100,000 µS/cm for the feed and permeate streams, respectively, in the form of a 4 – 20 mA current signal. The conductivity reading was converted to a measurement of TDS using equation (S.1). However, the relationship between electrical conductivity and TDS varies with water salinity. The conversion factor, K, was considered as 0.64 and 0.55 for feedwater and permeate water, respectively [4]. The feed and permeate conductivity sensors were calibrated using a NIST compliant conductivity standard solution of 12880 µS/cm. Their calibration data are included in Table S.3 in Section S.2.7.

$$C\ (mg/l) = Conductivity\ (\mu S/cm) \times K \quad \text{(S.1)}$$

Fig. S.8. Conductivity transmitter.

S.2.4 Temperature measurement

The feedwater temperature was measured using a temperature transmitter installed on the feed line of the RO system. The transmitter used is the TEAT-LL fluid temperature transmitter manufactured by SYXTHSENSE (Exeter, United Kingdom), shown in Fig. S.9. The sensor generated a 4 – 20 mA signal for a 0 to 50ºC temperature range. The sensor accuracy is ± 0.5ºC [5].

Fig. S.9. Temperature transmitter.

S.2.5 Power consumption measurement

The power consumption of each motor was calculated using equation (S.2), such that I_{Ph} is the current through a single phase, V_{Ph} is the phase voltage, and PF is the power factor of the respective motor. The phase voltage for each motor was constant at 240V before the VFDs and the power factor for each motor was supplied by the manufacturers. The phase current for each motor was measured using current sensors installed on single-phase lines before the VFDs and used to calculate the power consumption from equation (S.2). The current transmitter used are the HOBUT (Walsall, United Kingdom) CT132TRAN, shown in Fig. S.10. They generated a 4 – 20 mA signal for a current range of 0 – 10A, 0 – 20A and 0 – 50A, depending on the motor power, with an accuracy of ± 0.5% of the max current reading [6].

$$P = 3V_{Ph}I_{Ph}PF \tag{S.2}$$

Fig. S.10. Current transmitter.

S.2.6 Experimental error

Table S.2.

Estimation of experimental error

Measurement	Instrument	Error
Flowrate	OMEGA - FPB151 paddle wheel flowmeter	± 1% of the max reading
Pressure	RS PRO IPS Series pressure sensors	±0.25% of the max reading
Concentration	OMEGA - CDTX-2854 conductivity transmitter	±2% of reading
Temperature	SYXTHSENSE - TEAT-LL fluid temperature transmitter	± 0.5ºC
Electric current	HOBUT CT132TRAN	± 0.5% of the max reading

S.2.7 Conductivity sensors calibration

The feed and permeate conductivity sensors were calibrated based on a single-point calibration using a 12,880 μS/cm NIST compliant conductivity solution.

Table S.3.

Conductivity sensor calibration.

Sensor	Target value (μS/cm)	Sensor reading (μS/cm)	Actual Error (% of reading)	Rated accuracy (% of reading)
Feed conductivity	12,880	13078.9	+1.54	±2%
Permeate conductivity	12,880	12987.7	+0.84	±2%

S.3 References

1. Omega. *FPB100 series paddlewheel flow meter*. 2021 [cited 2021 September]; Available from: https://www.omega.com/en-us/flow-instruments/flow-meters/paddlewheel-flow-meters/p/FPB100-Series.
2. RS-components. *RS PRO IPS Series pressure sensors*. 2021 [cited 2021 September]; Available from: https://uk.rs-online.com/web/p/pressure-sensors/7975005/.
3. Omega. *CDTX-2851 Integral mount conductivity transmitters*. 2021 [cited 2021 September]; Available from: https://www.omega.com/en-us/control-monitoring/air-soil-liquid-and-gas/water-quality-transmitters/cdtx-2850-series/p/CDTX-2851.
4. Walton, N.R.G., *Electrical Conductivity and Total Dissolved Solids—What is Their Precise Relationship?* Desalination, 1989. **72**(3): p. 275-292.
5. SYXTHSENSE. *TEAT-LL fluid temperature transmitter*. 2021 [cited 2021 September]; Available from: https://www.syxthsense.com/sensors/teat-ll/fluid-temperature-transmitter,-4..20ma/.
6. HOBUT. *HOBUT CT132TRAN current transmitter*. 2021 [cited 2021 September]; Available from: https://www.hobut.co.uk/ct132tran-current-sensor-current-transducer/.